Bull Volcanol (2002) 64:455–471
DOI 10.1007/s00445-002-0222-5

RESEARCH ARTICLE

**Alexander Belousov · Barry Voight
Marina Belousova · Anatoly Petukhin**

Pyroclastic surges and flows from the 8–10 May 1997 explosive eruption of Bezymianny volcano, Kamchatka, Russia

Received: 6 January 2000 / Accepted: 8 April 2002 / Published online: 23 July 2002

Abstract The 8–10 May 1997 eruption of Bezymianny volcano began with extrusion of a crystallized plug from the vent in the upper part of the dome. Progressive gravitational collapses of the plug caused decompression of highly crystalline magma in the upper conduit, leading at 13:12 local time on 9 May to a powerful, vertical Vulcanian explosion. The dense pyroclastic mixture collapsed in *boil-over* style to generate a pyroclastic surge which was focused toward the southeast by the steep-walled, 1956 horseshoe-shaped crater. This surge, with a temperature <200 °C, covered an elliptical area >30 km^2 with deposits as much as 30 cm thick and extending 7 km from the vent. The surge deposits comprised massive to vaguely laminated, gravelly sand (Md –1.2 to 3.7ϕ; sorting 1.2 to 3ϕ) of poorly vesiculated andesite (mean density 1.82 g cm^{-3}; vesicularity 30 vol%; SiO_2 content ~58.0 wt%). The deposits, with a volume of 5–15×10^6 m^3, became finer grained and better sorted with distance; the maximal diameter of juvenile clasts decreased from 46 to 4 cm. The transport and deposition of the surge over a snowy landscape generated extensive lahars which traveled >30 km. Immediately following the surge, semi-vesiculated block-and-ash flows were emplaced as far as 4.7 km from the vent. Over time the juvenile lava in clasts of these flows became progressively less crystallized, apparently more silicic (59.0 to 59.9 wt% SiO_2) and more vesiculated (density 1.64 to 1.12 g cm^{-3}; vesicularity 37 to 57 vol%). At this stage the eruption showed transitional behavior, with mass divided between collapsing fountain and buoyant column. The youngest pumice-and-ash flows were accompanied by a sustained sub-Plinian eruption column ~14 km high, from which platy fallout clasts were deposited (~59.7% SiO_2; density 1.09 g cm^{-3}; vesicularity 58 vol%). The explosive activity lasted about 37 min and produced a total of ~0.026 km^3 dense rock equivalent of magma, with an average discharge of ~1.2×10^4 m^3 s^{-1}. A lava flow ~200 m long terminated the eruption. The evolutionary succession of different eruptive styles during the explosive eruption was caused by vertical gradients in crystallization and volatile content of the conduit magma, which produced significant changes in the properties of the erupting mixture.

Keywords Explosive eruption · Pyroclastic surge · Pyroclastic flow · Lava dome · Fragmentation of magma · Bezymianny volcano · Kamchatka

Editorial responsibility: S. Carey

A. Belousov (✉) · M. Belousova
Institute of Volcanic Geology and Geochemistry,
Petropavlovsk-Kamchatsky 683006, Russia
e-mail: belousov@mail.ru
Fax: +7-95-1330520

A. Belousov
GEOMAR, 24148 Kiel, Germany

B. Voight
Department of Geosciences, Pennsylvania State University,
University Park, PA 16802, USA

A. Petukhin
Kamchatka Experimental
and Methodical Seismological Department,
Geophysical Survey,
Petropavlovsk-Kamchatsky 683006, Russia

Present address:
A. Petukhin, Geo-Research Institute, Osaka, 550-012, Japan

Introduction

Explosive activity accompanying the growth of silicic lava domes has been of concern to the scientific community since 1902, when a moderate eruption of Mt. Pelée on Martinique led to the total destruction of the town of St. Pierre and killed 27,000 people (Lacroix 1904). The devastation of St. Pierre was caused by a previously unrecognized volcanic phenomenon, the pyroclastic surge – a hot, dilute, extremely mobile pyroclastic density current in which particles are carried in turbulent suspension and in a thin bed-load layer (Fisher and Heiken 1982; Druitt 1998). Pyroclastic surges can be generated by several processes and from eruptions of different types and

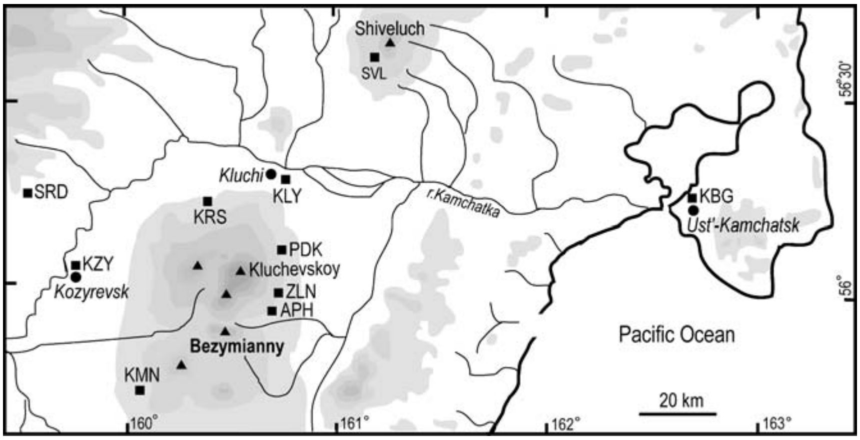

Fig. 1 Sketch map of the region of Kluchevskaya group of volcanoes (*triangles*) and locations of seismic stations (*squares*): *APH* Apahonchich (station closed in 1986), *ZLN* Zelionaya, *KMN* Kamenistaya, *KLY* Klyuchi, *KZY* Kozyrevsk, *KRS* Krestovsky, *KBG* Krutoberegovo, *PDK* Podkova, *SVL* Shiveluch, *SRD* Sredinny. Stations KZY and KLY are located in the towns Kozyrevsk and Klyuchi (*circles*), respectively, from which most of the visual observations of the May 1997 eruption were carried out. Only active volcanoes, with the exception of Kamen, are indicated. *Shaded areas* represent different elevations with 500-m steps

magnitudes. Surge-generating eruptions can be phreatic, phreato-magmatic or magmatic, and range in scale from relatively weak to violent (Sheridan and Wohletz 1983; Fisher and Schmincke 1984; Cas and Wright 1987; Carey 1991; Francis 1993; Macias et al. 1997, 1998; Druitt 1998; Wohletz 1998; Valentine and Fisher 2000). Hence, surges exhibit a wide range of velocities, temperatures, particle concentrations, and moisture contents, resulting in different flow and depositional processes, and consequently in diverse characteristics of deposits.

Three main classes of pyroclastic surges can be distinguished: (1) surges detaching from parental pyroclastic flows (ash-cloud surges and ground surges; Carey 1991; Sparks et al. 1997; Abdurachman et al. 2000), (2) directed-blast surges generated by decompression of internal parts of domes, cryptodomes and conduits as a result of large-scale slope failures (Hoblitt et al. 1981; Kieffer 1981; Druitt 1992; Belousov 1996; Sparks et al. 2002), and (3) base surges originating directly by fallback of near-vertical explosion fountains or from continuous fountaining (Taylor 1958; Moore 1967; Sigurdsson et al. 1987; Hoblitt et al. 1996; Macias et al. 1997; Druitt et al. 2002; Clarke et al. 2002).

Here we report the results of our investigation of pyroclastic deposits of the 8–10 May 1997 eruption of Bezymianny volcano (Kamchatka, Russia), which included a powerful pyroclastic surge produced by collapse of a vertical explosion fountain. This was one of the most important eruptions of Bezymianny since the gigantic directed blast of 1956 (Gorshkov 1959; Belousov 1996), comparable in explosivity only with the 1985 eruption (Alidibirov et al. 1990b). The scale of the surge was similar to that generated at Mt. Pelée on 8 May 1902.

History of Bezymianny lava dome eruptions

Bezymianny is one of a cluster of active volcanoes forming the Kluchevskaya group near the northern end of the Eastern volcanic belt of the Kamchatka peninsula (Figs. 1 and 2). The volcano forms an andesitic edifice approximately 3,000 m high, superimposed on the southeastern foot of the extinct Kamen volcano, 4,580 m high (Bogoyavlenskaya et al. 1991).

After approximately 1,000 years of dormancy (Braitseva et al. 1991), the first historical eruption of Bezymianny commenced in October 1955, and the climactic explosive eruption occurred on 30 March 1956 (Gorshkov 1959; Belousov 1996). Soon afterward the formation of the andesitic lava dome named *Novy* (meaning "new") started in the newly formed, 1.5-km-diameter, horseshoe-shaped crater which opened toward the southeast. Further dome growth followed, and by 1976 the dome volume had reached 0.36 km^3 (Seleznev et al. 1984). After that, the dome volume – although it fluctuated – did not change substantially because the parts of the dome destroyed by explosive eruptions were replaced soon afterward by extruded lava coulées of comparable volumes.

In the first few years after 1956, lava extruded more or less continuously, and spines were formed on occasion at different locations on the surface of the dome. Intermittent growth has occurred since 1965 and, in addition to episodic extrusion of stiff spines, extrusions of plastic lava also began to occur, although the magma composition did not change substantially (Bogoyavlenskaya and Kirsanov 1981; Alidibirov et al. 1990b). Viscosity of the lava fluctuated but in general decreased gradually with time and, during the last two decades, this was reflected in the extrusion of several, comparatively long lava flows to a distance of 0.7 km from the vent (Belousov et al. 1999). Also after 1965, coincident with the general decrease of viscosity of the extruded lava, eruptive processes became focused in a single vent in the upper part of the dome (Seleznev et al. 1984).

Since 1956 the dome growth has been accompanied by moderate explosive eruptions, and about 33 explosive events were recorded before 1997 (Simkin and Siebert 1994; Belousov et al. 1999). Within the last two decades, eruptions have occurred once or twice a year. They have developed (with some variations) with a generally similar pattern, the most common scenario being as follows.

1. The eruptive process begins with the slow extrusion of a relatively low-temperature, fully crystalline spine (plug) from the vent. Parts of the spine collapse from time to time, forming rock avalanches on the flanks of the dome. The frequency of rock avalanche occurrence gradually increases over periods of days to weeks. At first they are relatively cold (subsolidus temperature) but, as deeper, hotter parts of the plug are extruded, the rock avalanches start to resemble small-scale Merapi-type block-and-ash pyroclastic flows (Francis 1993; Abdurachman et al. 2000; Voight et al. 2000).
2. Within several days to weeks the eruption suddenly develops into an explosive phase which lasts several hours to days. Commonly, explosions through the upper part of the dome produce a vertical eruptive cloud as high as 15 km, and fountain collapse generates typically narrow, block-and-ash pyroclastic flows which travel 4 to 7 km, and rarely, as in 1985, to 12.5 km along the southeastern flank of the volcano. Billowing ash clouds override these pyroclastic flows and produce small-scale ash-cloud surges which travel not more than a few hundred meters from the parental pyroclastic flows.
   Since 1984, slope failures of old parts of the dome commonly accompanied the explosive eruptive phases. Material from the dome collapses intermixed with explosively generated pyroclastic flows. The resulting block-and-ash pyroclastic flow deposits sometimes contained more than 50% of clasts of old dome lava, which commonly had a distinctive reddish color due to oxidation, and was denser than the juvenile andesite of the pyroclastic flows. The largest collapse of the dome occurred in 1985, with a volume ~6×10^6 m^3, and was accompanied by the strongest of the post-climactic explosive eruptions (Alidibirov et al. 1990a, 1990b). This dome collapse caused decompression of the dome interior, and resulted in an explosively generated pyroclastic surge (lateral blast) of moderate size which traveled as far as 5 km from the dome.
3. The explosions produce a crater-like depression in the upper surface of the dome from which, after the end of the explosive phase, effusion of viscous lava typically occurs over periods of several days to months. Lava partially or completely fills in the crater and repairs the local scars formed as a result of slope failures of the dome. The longest lava flow (~700 m) effused in 1994–1995 (Belousov et al. 1999).

Although the above general scenario is most common, many variations have occurred over the history of numerous eruptions. In some cases effusion of lava preceded the explosive phase, as in 1986, or an explosive phase did not occur at all, as in 1986–1987. In other cases, as in 1990 and 1996, prolonged effusions of lava were not accompanied by explosive activity (Zharinov et al. 1991; Belousov et al. 1996).

The last explosive eruption detected prior to the 8–10 May 1997 eruption occurred on 6–8 October 1995 (Ozerov et al. 1996). According to seismic data the explosive activity consisted of three short pulses on 6 October 1995, and another on 7 October. The only observed eruption plume was generated by the second pulse and rose 5 km above the dome. The volcano was not visited after that eruption, and the eruption products were not studied. In August 1996, a lava flow was extruded but the eruption was not accompanied by explosive activity (Smithsonian Institution 1996).

Observational and seismological data of the 8–10 May 1997 eruption

Visual data about the course of the May 1997 eruption are scarce and incomplete because the volcano is located in an uninhabited area, and is visible only from distal settlements and from sides inconvenient for observations. Most observational data concerning this eruption have been summarized by the Bulletin of the Smithsonian Institution, together with information gathered from weather satellites (Smithsonian Institution 1997; NOAA, personal communication). Seismic signals of the eruption were recorded by the telemetered network of the Russian Geophysical Survey (Fig. 1).

Reactivation of the volcano probably commenced about 19 April 1997 when the seismic station Zelionaya (ZLN, 14 km from the volcano, Fig. 1) began to detect very low tremor (peak velocity ~0.1 μm s^{-1}). Three weak, shallow earthquakes on 27 April and four more on 8 May were recorded by ZLN only; they were attributed to Bezymianny by their waveforms. Tremor had build up to 0.75 μm s^{-1} by 8 May, with the continuous signal obscuring the recording of discrete earthquakes. By analogy with the previous eruptive history, we suspect that the tremor and earthquakes were connected with the slow extrusion of a stiff spine through the upper part of the dome. The hot spot on satellite images detected on 8 May (Smithsonian Institution 1997) could have represented hot, rock avalanche deposits which fell from the spine.

The first plume of the eruption, about 4 km high, was witnessed from the town Klyuchi (KLY on Fig. 1) at 05:45 on 9 May (here and in the following, heights are given above the dome which is at approximately 3,000 m a.s.l., and time is local = UTC+13 h). By this time the plume extended 40 km southeast. The eruptive activity probably commenced at 03:40 when the tremor increased up to 3.8 μm s^{-1} at the ZLN seismic station. Then, the tremor decreased and the height of the plume waned to about 3 km but, at 13:12, the strongest explo-

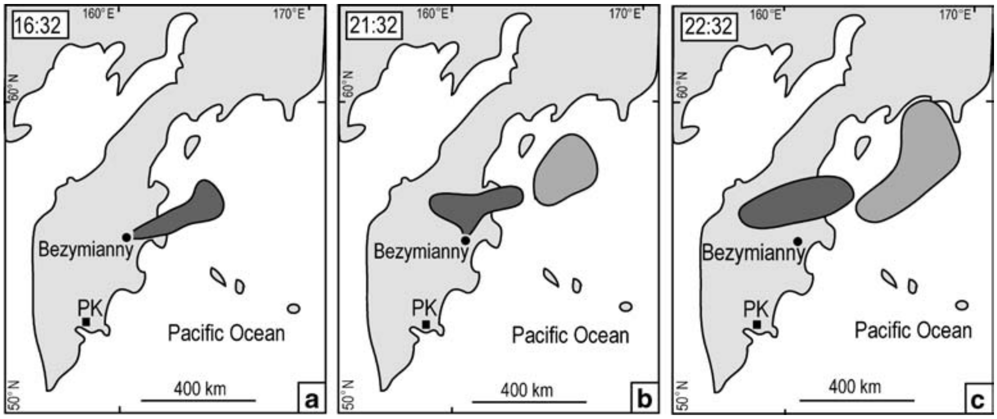

Fig. 2a–c Sketches of space images of volcanic clouds produced by the eruption of Bezymianny on 9 May 1997. **a** 16:32, **b** 21:32, **c** 22:32 LT (UTC+13 h). In **b** and **c** the clouds are subdivided into low-level (*dark gray*) and high-level (*light gray*) parts. *Closed circle* Location of Bezymianny volcano, *PK* Petropavlovsk-Kamchatsky

sion of the eruption occurred and produced an eruption column 12–14 km high, observed from Kozyrevsk (KZY) and Klyuchi (KLY; Fig. 1; Smithsonian Institution 1997). This plume drifted north-northeast and, at 16:30, ash began to fall in the town of Klyuchi where 180 g m^{-2} accumulated over the following 2 h. Satellite images acquired at 16:32 indicated the plume extended 400 km east-northeast (Fig. 2a). The explosion at 13:12 was characterized by an abrupt increase of tremor amplitude by several hundred times (Fig. 3a). The tremor remained at peak level for about 2 min and then decreased, but it continued at intensive level for the following 35 min. It saturated the two nearest seismic stations (ZLN and PDK) during the intervals of intense tremor amplitude, and was recorded by all other regional stations (Figs. 1, 3). The initial, strongest pulse of the tremor (at ~13:12–13:14) had ground peak velocities about 10 times higher than tremors from all previous major eruptions of Bezymianny since 1977 (Fig. 3b). These data confirm the unusually strong explosive event at the beginning of the 9 May 1997 explosive eruption. Intensity of the tremor after the initial peak (~13:14–13:49) was comparable with the tremor intensities recorded in previous eruptions (V.T. Garbuzova, personal communication; Ozerov et al. 1996).

Seismic activity declined substantially after this episode. At 21:32 satellite images showed the plume extended 600 km east-northeast, with the leading high-level plume sheared from the proximal low-level plume attached to the volcano (Fig. 2b). At 22:32 satellite images showed that the low-level plume was also detached from the volcano, indicating that explosive activity had waned (Fig. 2c). By about 03:00 on 10 May, observations from Klyuchi indicated the plume was 6 km high and, soon after that, the plume generation ceased.

Before the eruption, the vent of the dome had been completely infilled by solidified lava which had been extruded after the previous explosive eruption in 1995 (Ozerov et al. 1996; Smithsonian Institution 1996). When our field expedition visited the volcano in August 1997, we discovered that the May explosive activity had destroyed the top of the dome, forming a funnel-shaped crater ~200 m across, breached to the southeast (Fig. 4).

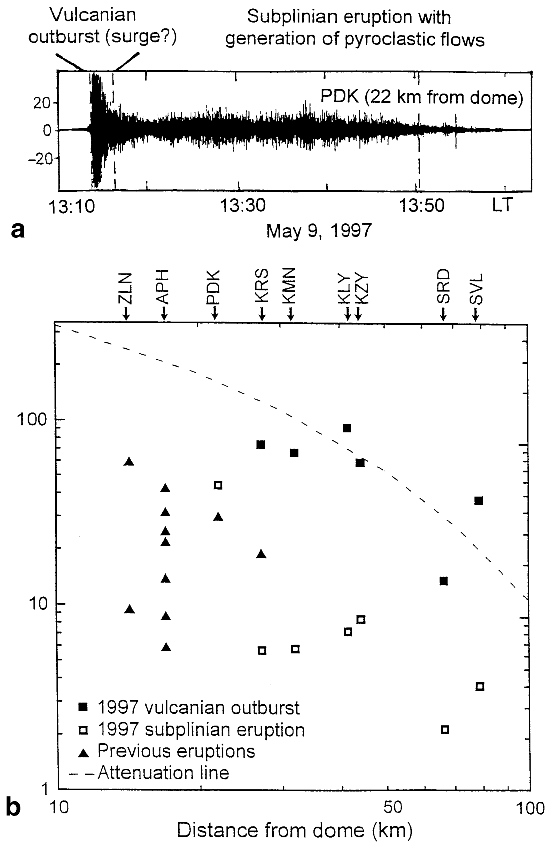

Fig. 3 **a** Example of the record of volcanic tremor related to the climactic stage of the 9 May 1997 Bezymianny eruption at Podkova seismic station (*PDK*), as shown in Fig. 1. Strongest tremor in the beginning of the records is interpreted to correspond to the powerful initial explosion during which the surge was generated. **b** Peak velocities of volcanic tremor (μm s^{-1}) of several recent eruptions of Bezymianny. Note the logarithmic scale of tremor intensity, showing that the initial phase of the 9 May 1997 eruption generated tremor an order of magnitude stronger than previous eruptions of the volcano. Stations closer than *PDK* were oversaturated by the initial phase of this eruption. The following phase, interpreted to represent the pyroclastic flow generation and sub-Plinian phase of the eruption, is comparable in tremor velocities to previously recorded events

Fig. 4 Bezymianny volcano after the May 1997 eruption. View from the east, taken in August 1997. The funnel in the upper part of the dome was formed during the explosive phase of the eruption. After the explosive phase a short lava flow effused from the funnel breach on the eastern part of the dome. Walls of the 1956 horseshoe-shaped crater directed the 1997 surge to the southeast (toward the reader). The diameter of the crater (~1.5 km) gives the scale

From the crater a short flow (~200 m) of degassed lava had been extruded to terminate the eruption.

Pyroclastic deposits of the 1997 eruption

Pyroclastic products of the eruption are represented by successively emplaced *pyroclastic surge*, *pyroclastic flow* (with associated minor *ash-cloud surges*), and *fall-out* pumice deposits (Fig. 5a, b). Stratigraphic relations between all the deposits cannot be observed in a single outcrop, but they can be inferred easily from a number of locations where deposit contacts are clearly visible.

Pyroclastic surge deposit

The surge deposit was found on the three ridges spreading radially from the volcano to the southeast, a direction which corresponded with the breach of the 1956 horseshoe-shaped crater (Fig. 5b). Although we did not visit the northern and western slopes of the volcano, observations from helicopter indicated no significant surge deposits in these sectors. Obviously, in these directions, the surge current had been blocked by the high scarp of the 1956 collapse crater, and much of the radial surge current was redirected by these crater walls toward the southeast. In valleys between the radial ridges, the surge deposit was almost immediately removed by incorporation into an extensive and voluminous lahar which was generated subsynchronously with surge deposition. The lahar was generated rapidly by the erosive impact of the hot surge on several meters of snow which had accumulated over the winter period on the flanks of the volcano, and also in the moat between the dome and the walls of the 1956 crater. Generation of the lahar by rapid mixing of the hot surge with melted snow explains the similarity of the grain-size distributions and clast compositions of the lahar and the surge deposit (see below). The lahar traveled more than 30 km down the broad valleys of the Tundrovy Klutch and Sukhaya Khapitsa rivers (Fig. 5b).

The pyroclastic surge blanketed an elliptical area of 30 km², extending as far as 7 km southeast from the cra-

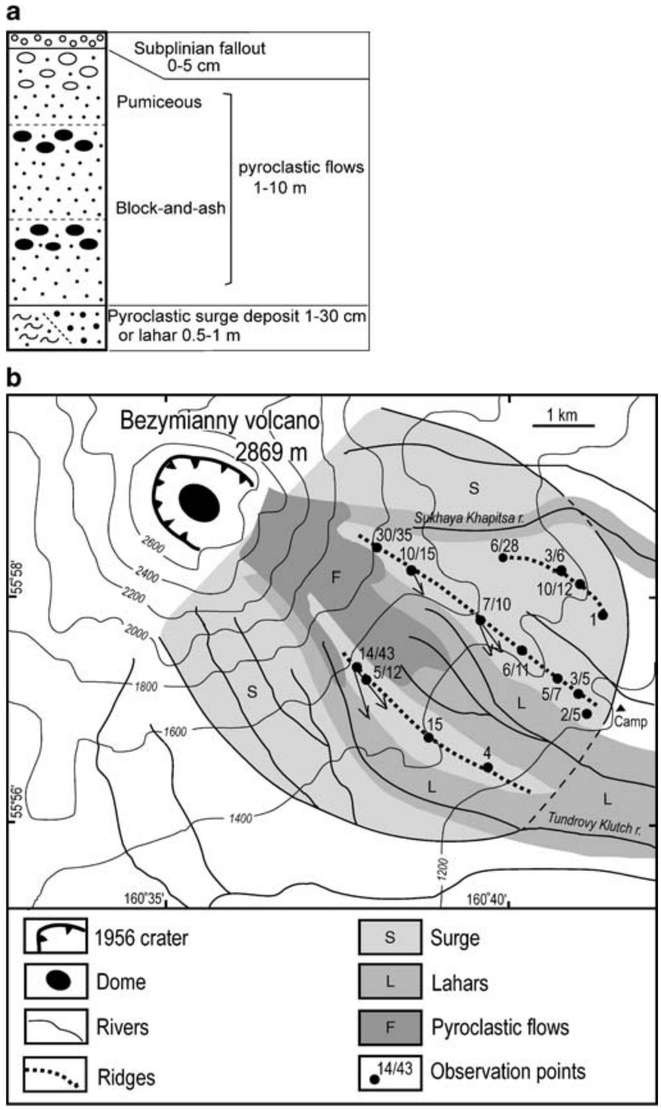

Fig. 5 a Composite stratigraphic section of deposits of the 8–10 May 1997 eruption of Bezymianny volcano. **b** Sketch map of deposits of the 8–10 May 1997 eruption of Bezymianny volcano. Deposits of fallout and ash-cloud surges are not shown. Surge deposit was studied mostly along the crests of ridges (unofficial names Northern, Camp, and Southern from north to south accordingly). Between the ridges the surge deposit was removed by subsynchronous lahars. *Numbers* near each site correspond to the thickness/maximum clast size of the surge deposit (in cm). If only one value is indicated, it corresponds to thickness of the deposit. *Arrows* indicate transport directions of fragments of the geodesic benchmarks destroyed by the 1997 surge. Dispersion of fragments appears to have been influenced by local topography, suggesting moderate current speed. Block-and-ash flows and pumice-and-ash flows are not subdivided on the sketch

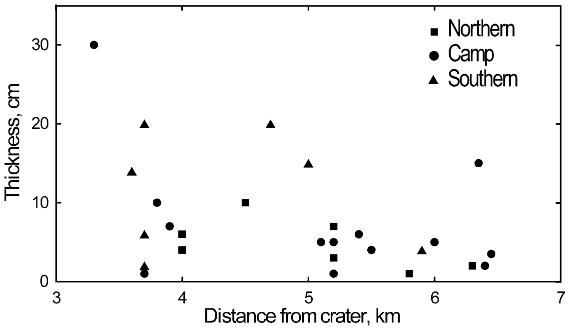

Fig. 6 Thickness of the 1997 surge deposits versus distance from the crater along the Northern, Camp and Southern ridges (unofficial names; for location of ridges, see Fig. 5b)

Fig. 7 Lightly shaded surge deposit (*S*) of the 9 May 1997 eruption resting on dark soil. Note large accidental clast on the surface of surge. Scale size is 13 cm. Location is site 7/10 on Fig. 5b, with distance from dome 5.1 km

ter. The slope inclinations decreased from about 35° on the apron of the dome to 6° near the distal boundary of the surge. The thickness of the surge deposit is variable and declines both toward the ridge crests and with distance from the source (Fig. 6). The maximum observed thickness of the deposit was 30 cm at a site 3.2 km from the dome; it decreased to about 1 cm on the outer boundary of the area affected by the surge. Local fluctuations of thickness were gradual and may have been related topography. We presume that a thicker and coarser facies of the surge was deposited in the valleys between the radial ridges, but most of this material was removed almost immediately by lahars.

The deposit had no areas of well-developed dunes. Several isolated, dune-like thickenings of the deposit (up to 30 cm above a background thickness of 2–3 cm) were found only near small-scale topographic irregularities near the ridge crest, where the surge current may have formed sustained vortices.

As the deposit was of strongly variable observed thickness, and entrainment and re-deposition of much of the deposit by lahars, the volume of the surge deposit could be only roughly estimated, as $5–15\times10^6$ m^3 (~$4–10\times10^6$ dense rock equivalent, DRE). The actual volume erupted must be larger than this value, because in the estimate above we do not include fines elutriated in the co-surge ash cloud (typically ~20–40%) and deposited downwind (Sparks and Walker 1977). Likewise, we do not include in the volume estimation any surge deposits trapped within the moat of the 1956 crater.

Several geodesic benchmarks were damaged or destroyed by the surge, and their wood fragments showed no traces of thermal impact. Hence, we conclude that the temperature of the surge cloud deposits was <200 °C, i.e., much lower than magmatic temperatures of around 900 °C (Ivanov et al. 1978); cooling was induced by entrained cold air and eroded snow. The sides of the wood benchmark structures which faced toward the volcano were abraded and pitted. Fragments of the destroyed benchmarks were transported by the surge to distances as far as several hundred meters along the azimuths 135–160° (arrows on Fig. 5b). These directions suggest a role of local topography in movement of the surge.

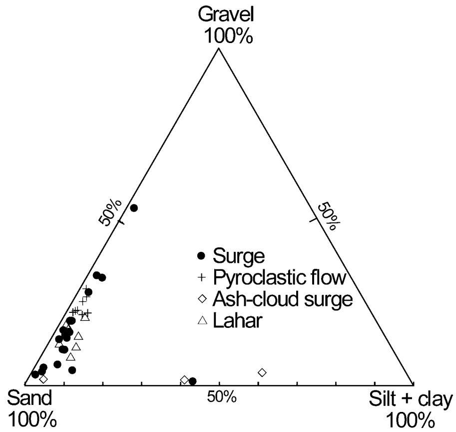

Fig. 8 Percentage of gravel (>2 mm), sand (0.063 to 2 mm) and silt+clay (<0.063 mm) in the 8–10 May 1997 deposits of Bezymianny volcano. Only the matrix of pyroclastic flows was analyzed, as the pyroclastic flows included boulder-size material. Grain-size characteristics of the lahar deposits are similar to those of the surge deposit, and reflect an origin from surge-snow interaction

The surge deposit is represented by massive to vaguely laminated, relatively well-sorted gravelly sand (for descriptive characterization of grain sizes, we use the convenient sedimentary terms "gravel", "sand, "silt" and "clay"; Figs. 7, 8, 9; Table 1). On a plot of sorting versus median diameter, most of the deposit samples occupy the area, common for pyroclastic surges, for the overlapped fall and flow fields (Fig. 9). Grain-size distributions of the deposit are commonly unimodal, with a well-developed mode at about 1–2ϕ. Samples taken in the proximal zone have an additional coarse-grained, gravel mode (Fig. 10). The deposit became finer grained by progressive loss of clasts larger than about 1 mm (coarse-tail grading), and better sorted with distance from the source (Figs. 10, 11a, b).

The largest clasts rested on the upper surface of the deposits. Juvenile gravel-sized clasts were equant to ob-

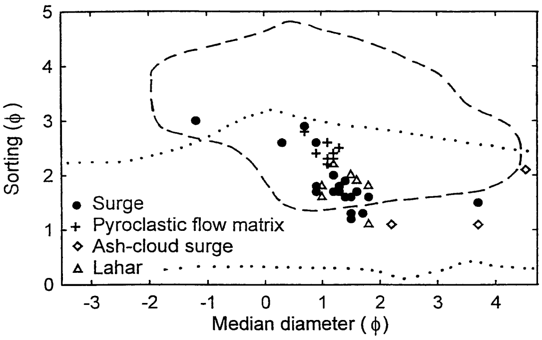

Fig. 9 Relationship between sorting and median diameter (coefficients after Inman 1952) for the 8–10 May 1997 deposits of Bezymianny volcano. *Dashed* and *dotted lines* outline areas of pyroclastic flow and fallout deposits, respectively (after Walker 1971)

Table 1 Granulometric characteristics of the 8–10 May 1997 deposits of Bezymianny volcano (sorting and median diameter after Inman (1952); *gravel* <–1ϕ (>2 mm), *sand* –1 to +4ϕ (2–0.063 mm), *silt+clay* >4ϕ (<0.063 mm), phi (ϕ) = $-\log_2$ diameter in mm). *n* Number of analyses

	Md (ϕ)	Sorting (ϕ)	Gravel (%)	Sand (%)	Silt+clay (%)
Surge (*n*=19)					
Range	–1.2–3.7	1.2–3	0.1–30.9	46.2–96.3	1.6–43.0
Average	1.2	1.9	14.9	79.3	5.8
Block-and-ash flow (*n*=3)					
Range	0.7–1.2	2.4–2.8	21.2–27.6	70.5–76.0	1.9–3.2
Average	0.9	2.5	24.7	72.7	2.7
Pumice-and-ash flow (*n*=6)					
Range	1.1–1.3	2.2–2.6	19.9–23.8	73.3–76.6	2.0–5.9
Average	1.2	2.4	21.3	74.8	3.6
Ash-cloud surge (*n*=3)					
Range	2.2–4.5	1.1–2.1	0.5–2.7	37.6–94.9	4.3–59.7
Average	3.5	1.5	1.3	63.7	34.9
Lahar (*n*=7)					
Range	1.0–1.8	1.6–2.2	7.5–19.3	74.5–85.5	2.0–8.3
Average	1.3	1.9	13.6	81.1	5.3

late (Fig. 12), with edges notably smoothed by abrasive rounding from particle interaction during energetic transportation in the surge cloud. Maximal diameter of juvenile clasts decreased from 46 to 4 cm with distance away from the source (Fig. 11c). In many locations a characteristic feature of the deposit surface was the presence of abundant, angular accidental boulder-size clasts which were notably larger than the nearby juvenile clasts (Figs. 7, 11c). These clasts were set into motion from the underlying ground surface, and rolled or slid over the thin deposits for distances of tens to hundreds of meters.

The clasts of juvenile two-pyroxene andesite (~58.0% SiO_2) in the surge deposit were poorly vesiculated, with measured density ranging from 1.74 to 1.90 g cm^{-3} (average 1.82 g cm^{-3}) and an average vesicularity of about 30 vol% (Table 2). The densities and vesicularities were

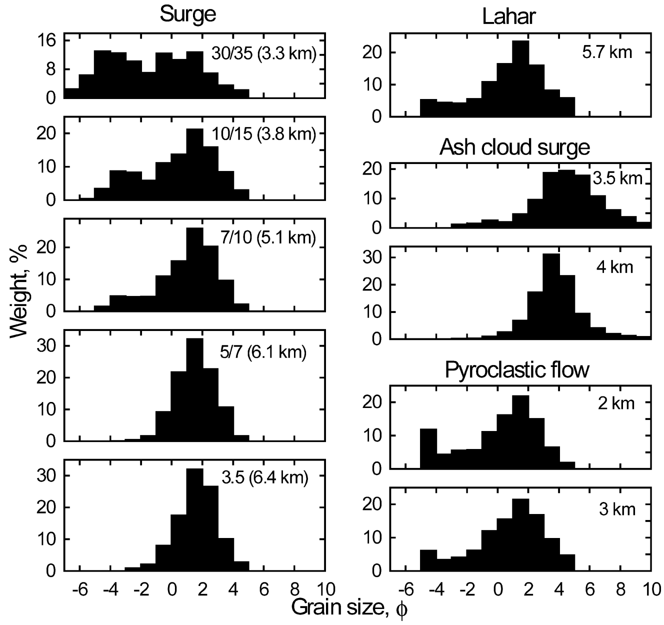

Fig. 10 Typical grain-size histograms of the 8–10 May 1997 deposits. Distances from crater are indicated. The *number* near each site corresponds to thickness/maximum clast size of the deposit (in cm; Fig. 5b). If only one value is indicated, it corresponds to thickness of the deposit. Location of sites are shown in Fig. 5b

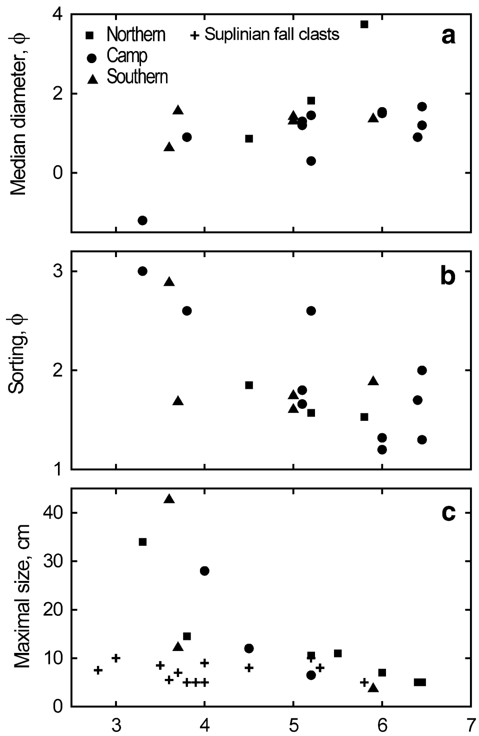

Fig. 11a–c Median diameter (**a**), sorting (**b**) and maximum size of juvenile clasts (**c**) of the 1997 surge deposits versus distance from the crater along the Northern, Camp and Southern ridges (for location of ridges, see Fig. 5b). Maximum size is defined as the mean value of the longest axes of the 10 largest clasts in an area of about 20×20 m

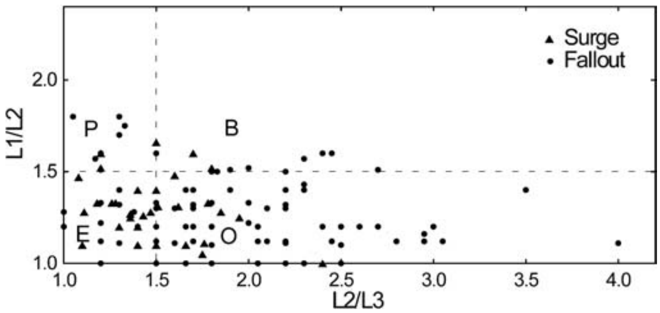

Fig. 12 Zingg diagram of clast shape for surge (*triangles*) and fallout (*circles*) deposits of the 8–10 May 1997 eruption. The fields *E*, *P*, *B*, *O* indicate fields of equant, prolate, bladed and oblate (disk) shape classes of Zingg (1935), respectively. Clast axes: L1=longest, L2=intermediate, L3=shortest. Note that the shape of many surge and fallout clasts is oblate

Table 2 Chemical compositions and densities of the products of the 8–10 May 1997 eruption of Bezymianny volcano. *N* Number of analyses

	Surge	Block-and-ash flow	Pumice-and-ash flow	Fallout
SiO_2 (wt%)[a]	58.0	59.0	59.9	59.7
Al_2O_3	18.0	17.7	16.3	17.0
TiO_2	0.76	0.78	0.84	0.78
Fe_2O_3	7.69	7.37	7.65	7.24
MnO	0.14	0.13	0.13	0.13
CaO	7.49	6.60	5.83	6.14
MgO	3.53	3.31	3.32	3.25
Na_2O	3.57	3.71	3.61	3.61
K_2O	1.25	1.48	1.63	1.53
P_2O_5	0.18	0.27	0.17	0.14
BaO	0.05	0.05	0.06	0.06
SrO	0.04	0.04	0.03	0.03
Total	100.6	100.4	99.5	99.6
Density (g/cm^3)				
Range	1.74–1.90	1.63–1.67	1.11–1.14	1.08–1.11
Average	1.82 (*n*=2)	1.64 (*n*=4)	1.12 (*n*=5)	1.09 (*n*=3)

[a] Major elements were measured by X-ray fluorescence in the Mineral Constitution Laboratory at Penn State University. Estimated analytical errors were calculated as percentages of amounts present: SiO_2, CaO, K_2O: <1%; TiO_2, Al_2O_3: 2%; MnO: 5%; MgO, Na_2O, P_2O_5: 3%

determined by the methods of Houghton and Wilson (1989) and Hoblitt and Harmon (1993). Percent vesicularity is defined by:

$$V\,(\%) = 100\ (DRE\ \text{density} - \text{clast bulk density}) / DRE\ \text{density}.$$

In our calculations, DRE density was taken as 2.6 g cm^{-3}.

The juvenile clasts were characterized by high crystallinity. Phenocrysts and microphenocrysts (>80 μm) comprise 71–86 vol% of solids, representing about 50–60 vol% of the bulk rock including pore space. Most clasts were vesicular, and two types of vesicles were distinguished (Figs. 13, 14).

Type 1. Large (0.1–0.5 mm), irregular, interconnected vesicles which were shaped by growth in the restricted spaces between closely situated phenocrysts. Commonly, inside these vesicles are thin (4–20 μm), long (100–150 μm) filaments of glass which connect the opposite sides of the vesicles.

Type 2. Small (3–20 μm), subspherical, isolated vesicles (bubbles) which probably were formed later than the type 1 vesicles; these grew in residual melt between large vesicles.

The morphology of juvenile andesite particles from the surge deposit (Fig. 14b) shows that they were formed by brittle fragmentation. Most silt-sized particles are angular, with the exception of rare clasts representing the surfaces of broken vesicles, or glass filaments. Sand-sized particles were typically irregular aggregates of phenocrysts bound together by a thin shell of glass. The surfaces of particles which contained remnants of former vesicles were smooth, but other surfaces were bounded by surfaces of cracks.

Component analyses of the fraction –1 to –2ϕ show that the surge deposit was composed of 47 to 92% (mean 79%) of juvenile andesite clasts. The remaining clasts comprised accidental heterolithological material which originated from older parts of the dome. This material includes pieces of lava dome or conduit included within the surge-producing explosion, and clasts of older deposits plucked by the surge cloud from the underlying ground surface.

The fact that the deposit is relatively well sorted, poor in fines, and consists of one thin layer with fine, internal wavy lamination shows that the surge represented a single short pulse of an inflated, hot, dry gas-pyroclastic mixture. An initially dry character of the surge cloud is supported by the lack of accretionary lapilli in the deposit. However, during the process of deposition the surge could have become progressively wet due to erosion and entrainment of snow from the substrate. We could not confirm this from study of the surge deposit itself, but in several locations we found transitions of the surge deposit directly into deposits of lahars. The surge cloud was probably formed by collapse of the powerful vertical fountain of a Vulcanian explosion, which occurred at 13:12 on 9 May when strongest tremor was registered during two minutes (Fig. 3a).

Pyroclastic flow deposits

Following the surge, pyroclastic flows, which traveled up to 4.7 km from the crater, were generated by eruption fountain collapse (Fig. 5a, b). They left deposits in the valleys of the southeast flank of Bezymianny, and on the strongly eroded surface left behind by the lahars which had been generated by the earlier pyroclastic deposition on the thick snow pack. The first were erupted flows of the *semi-vesicular block-and-ash* type (classification of

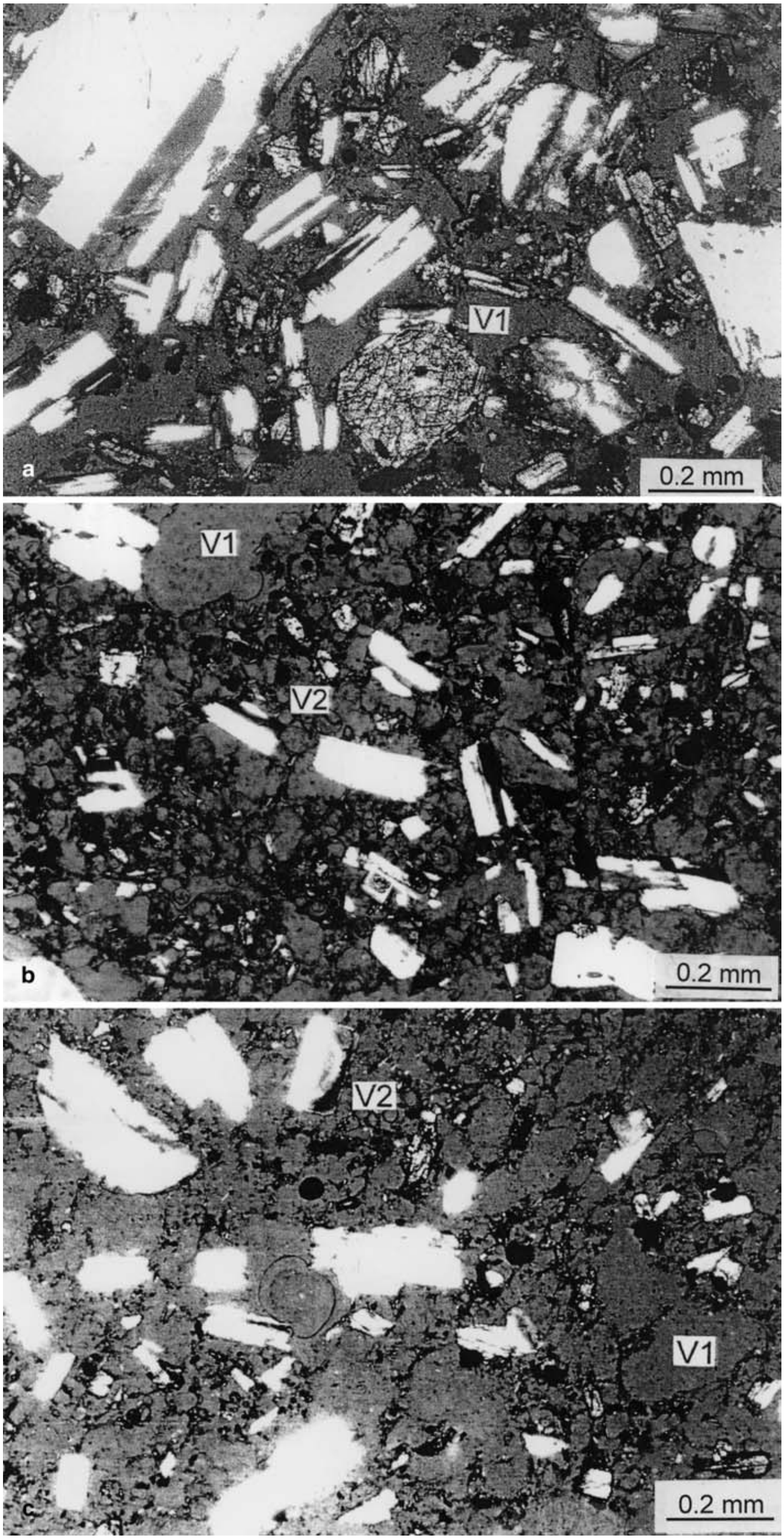

Fig. 13a–c Thin sections of andesite from successively erupted **a** surge, **b** pyroclastic flow, and **c** fallout deposits. Note strong decrease in crystallinity and increase in vesicularity from surge to fallout. *V1* and *V2* indicate vesicles of type 1 and type 2, respectively (see text for description). On the image of surge andesite (**a**), the type 2 vesicles are too small to be visible. Nicols are partially crossed to show vesicles

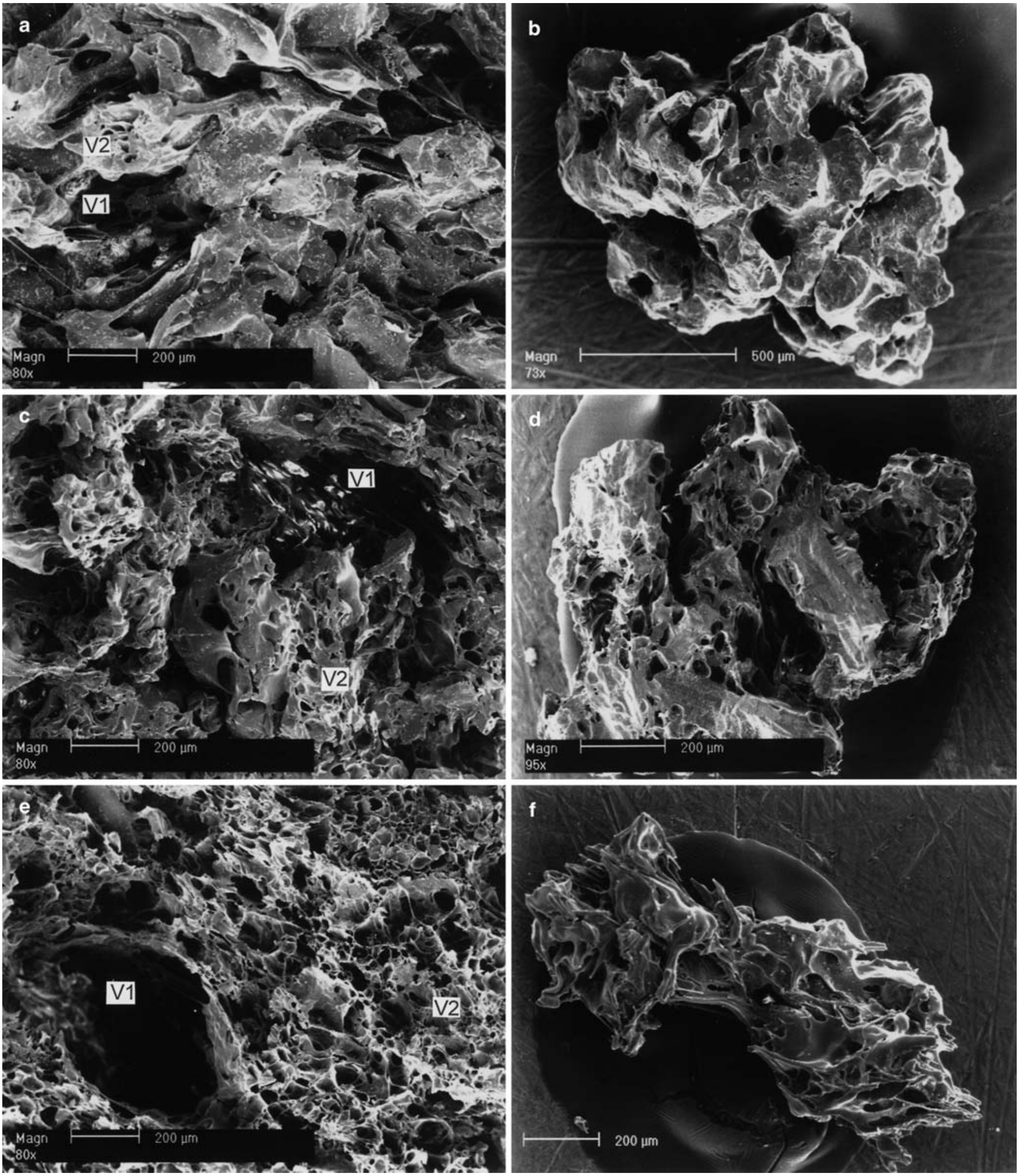

Fig. 14a–f SEM images of products of the 8–10 May 1997 eruption. **a**, **b** Surge. **c**, **d** Early block-and-ash flows (poorly vesiculated andesite). **e**, **f** Late pyroclastic flows (pumiceous andesite). **a**, **c**, **e** show the structure of andesite, and **b**, **d**, **f** the shapes of sand-sized particles. *V1* and *V2* indicate vesicles of type 1 and type 2, respectively. Note thin filaments of glass in type 1 vesicles of the surge

Smith and Roobol 1990), but *pumice-and-ash flows* were erupted later in the sequence. The deposits covered an area of about 5 km^2, the average thickness of individual flow deposits being about 3–5 m. Lobes of the individual pyroclastic flows had steep, bouldery fronts where maximum thicknesses of 10 m were observed. The individual clasts attained a maximum ~4 m diameter. Fresh fractures in large clasts were crossed by long filaments of rhyolitic glass, which confirmed the existence of some melt phase at the time of disruption and emplacement.

The grain-size characteristics of the matrix (boulder-size clasts could not be sampled) of these pyroclastic flows are generally similar to those of the proximal surge deposits (Figs. 8, 9, 10; Table 1). Component analyses of the clast fraction –1 to –2ϕ showed that, compared with the surge deposit, the flows were enriched in accidental material, juvenile clasts comprising 43–75% (mean 59%). This enrichment of accidental material was probably caused by vent erosion and localized failures of old parts of the dome during the eruption, and by erosion and entrainment by pyroclastic flows of old dome fragmental debris on the underlying surface. Our limited sampling suggested that subangular clasts of the semi-vesicular, juvenile andesite blocks in the pyroclastic flows were slightly less dense and more vesicular than clasts of the surge (densities 1.64 versus 1.82 g cm^{-3}, and vesicularities 37 versus 30 vol%, respectively).

The clasts of juvenile lava in the successive pyroclastic flows became progressively and gradationally more vesiculated (density 1.64 to 1.12 g cm^{-3}; vesicularity 37 to 57 vol%) and less angular (Figs. 13, 14; Table 2). Evidently they also became slightly more silicic (59.0 to 59.9 wt% SiO_2), although we caution that this comparison is based on only a few samples. The youngest pyroclastic flow deposits were characterized by pale gray, rounded clasts of andesite pumice and ash. The content of phenocrysts and microphenocrysts in these samples was notably less than in the andesite of the surge (~50 vol% of solids, representing about 30–20 vol% of the bulk rock depending on vesicularity). Overall, the mineral compositions of the semi-vesicular and pumiceous andesite clasts in the pyroclastic flows were similar to those documented in the andesite clasts of the surge deposit.

The volume of the pyroclastic flow deposits was estimated approximately as 20×10^6 m^3 (~13×10^6 m^3 DRE). Material possibly trapped within the 1956 crater moat is excluded in this calculation.

SEM images show that the two types of vesicles distinguished in material of the surge are also present, with some modifications, in the juvenile clasts of the pyroclastic flows (Fig. 14c, d). Vesicles of type 1, with diameters of 200–400 μm, are more equant in pyroclastic flow material because their growth was less restricted by phenocrysts and microphenocrysts. This is consistent with the lower crystallinity of the andesite clasts in pyroclastic flows. The progressive increase of total vesicularity over time of the erupted material occurred mainly due to a progressive increase of the number and size (up to 50 μm) of vesicles of type 2. In clasts from the early, semi-vesiculated block-and-ash flows, type 2 vesicles are still separated one from another by thick walls but, in clasts from the later pumice-and-ash flows, the inter-bubble walls are very thin and frequently disrupted. In accord with these systematic changes in properties of the erupted juvenile material, the morphology of sand-sized particles gradually changed due to increase in degree of vesiculation.

Lobes of the pyroclastic flow deposits are surrounded by thin (up to 20 cm) fine-grained ash deposits which we interpret as associated ash-cloud surges. The deposits extend less than 100 m from the margins of the parental flows. The deposits of the ash-cloud surges are better sorted and finer than those of the initial surge (Figs. 8, 9, 10; Table 1). The wide range of median diameters reflects a limited carrying capacity of the ash-cloud surges, and hence relatively quick fallout of coarse particles with distance beyond the parental pyroclastic flows.

The seismic data suggest that pyroclastic flow emplacement could have begun soon after the strong, surge-producing explosion at 13:12 on 9 May, when tremor with amplitudes more or less characteristic of previous eruptive activity was registered for about 35 min (Fig. 3a). Possibly the first flows were generated by the waning stage of the same explosion fountain which generated the initial surge of the eruption. Subsequent flows were generated by limited periodic collapse of the sub-Plinian column. On the whole these pyroclastic flows can be classified as a variety of St. Vincent type flows, although the classification is not completely adequate for the studied case.

Fallout

The axis of the fallout initially extended to the northeast, passing across the high summits of the Kamen and Kluchevskoy volcanoes (Fig. 1). The plume then separated, the low-level plume drifting to the north and the high-level plume moving northeast and out to sea (Fig. 2). The downwind distribution of tephra was not studied. To the southeast, in a direction normal to the fallout axis, widely scattered, angular fallout clasts of pumice up to 10 cm in diameter were deposited; their dimensions slowly decreased with distance from the vent (Fig. 11c). The pumice clasts were typically platy shaped (Fig. 12). These clasts fell out of the sub-Plinian eruption column which was observed after 13:12 on 9 May.

Because data about the distribution of thickness of fallout deposits are scarce, we estimate the volume of eruptive products from the empirical dependence between height of the eruption plume (H, in our case 14 km) and discharge rate of dense magma (Q) in m^3 s^{-1}:

$H = 1.67Q^{0.259}$ (Sparks et al. 1997)

Hence, the calculated value is Q=3,700 m^3 s^{-1} and, using the duration of strong volcanic tremor (35 min) to estimate the duration of the eruption, and allowing for fluctuations in intensity, we estimate the approximate volume erupted as fallout as 3×10^6 m^3 DRE.

The fallout tephra (59.7% SiO_2) is almost identical in overall petrology, crystallinity (~48 vol% solids), vesiculation and porosity (mean density 1.09 g cm^{-3}; vesicularity 58 vol%) to the clasts of the youngest pumice-and-ash flow deposits (Figs. 13, 14; Table 2). This strong similarity as well as stratigraphic relationships suggest that they were generated nearly synchronously in the sustained, explosive phase of the eruption. This phase of activity may be classified as a short-lived, sustained sub-Plinian eruption (Walker 1973).

Discussion

Inferred mechanism of eruption

Prior to the 1997 eruption, little seismic activity was observed which might have indicated the ascent of new magma from the magma reservoir. We suspect that the magma involved in the initial stages of the eruption was probably stored in the conduit at shallow depth, below a plug of crystalline lava. This magma may have ascended toward the surface at the end of the previous effusive eruption in August 1996, but was not erupted that time. During storage, volatile loss from the melt and slow cooling led to microphenocryst and phenocryst-rim crystallization of the magma (Sparks et al. 2000). Exsolution of volatiles during storage in the conduit resulted in large vesicles of type 1. This interpretation is consistent with the observations of vesicles and crystals in the earliest eruptive products of the May 1997 eruption. It is also consistent with the decompression experiments of Gardner et al. (1999) on bimodal size distribution of bubbles, which indicate that the population of bubbles grows during an eruption, but that larger bubbles may be either inherited from the region of magma storage or formed during coalescence. In our case we prefer the explanation of inheritance, because the high viscosity would have retarded independent bubble movement and coalescence.

Thus, immediately before the eruption, the conduit contained a crystal-rich viscous magma with a significant amount of volatiles (exsolved from the residual melt and accumulated under pressure in large vesicles of type 1) partly sealed under a crystalline plug. Some volatile leakage is considered likely. Magma deeper in the conduit was less crystalline and the residual melt was relatively volatile rich and, accordingly, its viscosity was much less. The melt composition was rhyolitic. Assuming a temperature range of about 900–930 °C and a water content of about 3 wt% (Ivanov et al. 1978), viscosity may have ranged from about 10^6 Pa s at depth to about 10^{14} Pa s for highly crystalline dome lava (cf. Hess and Dingwell 1996; Voight et al. 1999; Sparks et al. 2000). During the course of the eruption, these variations in the conduit magma resulted in an evolutionary succession of different eruptive styles and products. The degassing history is to some extent recorded by the vesiculation, although Gardner et al. (1996) note that this history is better recorded by the ratio of vesicle volume (gas) to glass (melt liquid) in vesicular clasts. At Bezymianny this gas/volume ratio varies from about 0.95 for surge clasts to about 1.8 for clasts of the pumice deposits, a variation of roughly a factor of two. The latter is near the minimum value recorded by Gardner et al. (1996) for pumices erupted in Plinian-type eruptions of viscous magma (>10^5 Pa s), and supports our interpretation of this sustained eruptive phase as sub-Plinian: we interpret the earlier, short-lived pyroclastic surge phase, with low gas/volume ratios, as Vulcanian.

We speculate that the eruption evolved as follows. In the beginning of the eruption, a buildup in magmatic overpressure resulted in the slow extrusion of the highly crystalline, upper part of the magma column, accompanied by shallow earthquakes and weak tremor. This is consistent with the previous eruptive history at Bezymianny (Alidibirov et al. 1990b), where nearly every eruption began with squeezing of blocks from the upper, active part of the lava dome. The degassed, solidified plug was slowly extruded at first, and collapsed in stages to produce small rock avalanches. Extrusion rate accelerated, and the later avalanches were hot and thus could explain the “hot spot” detected on the satellite images on 8 May. The largest of these block avalanches, similar to relatively small, Merapi-type block-and-ash flows (cf. Francis 1993; Voight et al. 2000), occurred early in the morning on 9 May and may have generated a pulse of seismic activity recorded at 03:40. Plumes observed at 05:45 may have been ash clouds rising from these flows.

Successive gravitational failures gradually destroyed the plug, leading to increased rate of extrusion, and ultimately to the explosive eruption by decompression of the gas-pressurized conduit. The ejecta assemblage is interpreted to have been derived from the conduit. The main lithological components erupted were not similar to older, dome-collapse pyroclastic flow deposits at Bezymianny, and typical dome-lava lithologies were rare in the ejecta. The semi-vesicular andesite, ejected in the opening vent-clearing explosions, originated from the upper part of the conduit. The pumice came from originally deeper parts of the conduit, in the subsequent sustained discharge involving volatile-enriched magma.

We infer that intense, vertical vent-clearing Vulcanian explosions occurred in the initial explosive stages, resulting in the generation of an immediately collapsing, “boil-over” fountain (Clarke et al. 2002). The dense pyroclast-gas mixture collapsed and moved radially as a pyroclastic surge, with much of the current then deflected toward the southeast by the steep walls of the 1956 horseshoe-shaped crater. We believe that fragmentation of the magma occurred mostly due to disruption of the large (type 1) vesicles. The low content of dissolved volatiles in upper conduit melt, the high crystallinity, and the high viscosity of the residual melt retarded vesiculation *during* the Vulcanian explosion and account for the scarcity of type 2 microvesicles in the surge clasts.

Less crystallized, deeper, and volatile-enriched parts of the conduit were then erupted in the form of block-and-ash flows fed by pyroclastic fountains, progressively involving lower-viscosity magma with a gradually larger fraction of volatiles dissolved in the residual melt. The higher melt volatile content and lower viscosity led to a progressive increase in size and number of type 2 microvesicles, and consequently the pyroclastic flows evolved from the initial block-and-ash type to pumice-and-ash flows. This part of the eruption showed transitional behavior in which mass was divided between a collapsing fountain and a buoyant plume, and the buoyant plume developed in strength to create a sub-Plinian column. Fallout from this column produced clasts nearly identical in texture and density to those found in the pumice-and-ash flows.

Eruption chronology

The surge-producing explosion was not directly observed and thus we cannot with certainty identify the period of its origin. However, stratigraphic information combined with the seismic data suggest that the surge-producing explosion occurred at ~13:12–13:14 on 9 May when, for two minutes, the tremor which was generated was far more energetic than those observed for any previous dome-forming eruption of Bezymianny. The 35 min of less intensive (but still strong) tremor which immediately followed this initial period is comparable with tremor of previous eruptions, and we attribute it to the formation of fountain-collapse pyroclastic flows and a sustained sub-Plinian eruption plume.

Strong explosive activity lasted about 37 min in all and produced roughly 0.026 km^3 DRE magma (sum of surge, flow and fall), with an average discharge of $\sim 1.2\times 10^4$ m^3 s^{-1}. The eruption is classed as VEI 3 (Newhall and Self 1982). The surge deposit and associated co-surge ash, nominally about 10×10^6 m^3 DRE, was erupted during the first 2 min, which suggests a flux of 8×10^4 m^3 s^{-1}. The pyroclastic flows and fallout tephra, with a total volume of $\sim 16\times 10^6$ m^3 DRE, were produced during the following 35 min, suggesting an average flux of about 8×10^3 m^3 s^{-1}.

Clast morphology

The oblate (platy) shape of many of juvenile clasts of the surge and fallout (Fig. 13) suggests that the conduit magmatic foam expanded by developing, through brittle fragmentation, a series of horizontal partings. The foamy material between the partings then separated to form tabular clasts. Shock tube experiments have shown that a fragmentation wave which propagates down into a volcanic conduit after rapid decompression can produce such tabular clasts (Anilkumar et al. 1993; Alidibirov and Dingwell 1996, 2000). We have observed such clast shapes in tephra from the 1994 eruption of the Kluchevskoy volcano, and in fallout pumice from vulcanian eruptions of the Soufriere Hills volcano, Montserrat (Druitt et al. 2002). Brittle fragmentation of vesicular magma would have required steep pressure gradients and fast decompression rates in order to drive the magma through the glass transition limit (Dingwell 1996, 1998). Magma fragments erupting from the vent apparently had high enough viscosities to suppress much post-fragmentation expansion, such that shapes acquired at fragmentation were more or less retained.

Evolution of chemical compositions

Apparently, the magma in successive stages of the eruption became progressively more silicic, with whole-rock SiO_2 contents increasing from ~58 wt% in surge deposit clasts to ~59 wt% in semi-vesiculated block-and-ash deposits, and to nearly 60 wt% in both the pumice-and-ash and sub-Plinian fallout deposits. We have only few chemical analyses, the XRF analytical precision is about 1%, and the specimens were highly crystalline, so we cannot exclude the possibility of an influence by random variations of crystal content in the samples analyzed. Nevertheless, the chemical variations are systematically gradational from one eruptive stage to the next, and this progression is consistent with stratigraphic relations and inferred eruption chronology, and also with gradational variations in vesicularity and crystallinity. Thus, we suspect the chemical gradation to be real, if puzzling, and not due to analytical variance.

Our results are consistent with the recent eruptive history at Bezymianny, where since 1956 a distinct periodicity of eruptive activity has been observed (Bogoyavlenskaya and Kirsanov 1981; Alidibirov et al. 1990b). Strong eruptions accompanied by pyroclastic flows occurred every decade or so, and brought less viscous magma of relatively low crystallinity to the surface. Then, in following years, the crystallinity increased by growth of microlites and subphenocrysts until a new batch of low-crystalline magma rose in the conduit to initiate a new cycle. Such distinct changes occurred in 1965 and 1976 (Bogoyavlenskaya and Kirsanov 1981), and in 1984–1985 (Alidibirov et al. 1990b) when violent explosions destroyed the upper part of the dome. The chemistry of the pumice in the May 1997 eruption is nearly identical to that of the 1956 Novy dome, marking the first return since that time of ~60 wt% SiO_2 compositions. Studies of the mineral and glass chemistry are underway and will be reported elsewhere.

Eruption analogs and surge generation mechanisms

The travel distance of the 1997 surge at Bezymianny is comparable with the travel distances of the famous surges of Mt. Pelée (1902) and El Chichon (1982), and only half as short as that of Lamington (1951). These were among the most destructive volcanic events of the 20th century (Fig. 15). The nature of the 1902 surge of Mt. Pelée is still under discussion (Fisher et al. 1980; Fisher and Heiken 1982; Boudon and Gourgaud 1989), and the processes at Lamington and El Chichon are also still being discussed and debated (Taylor 1958; Sigurdsson et al. 1987; Macias et al. 1997; Clarke and Voight 2000). At El Chichon, late-stage collapse of a plinian column

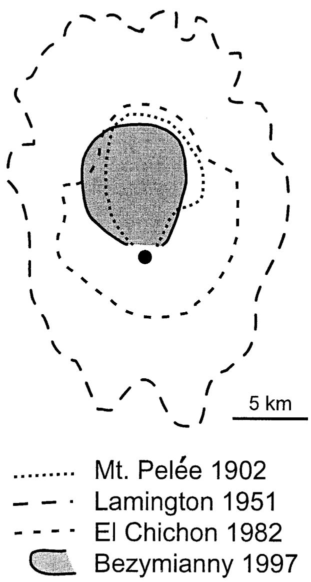

Fig. 15 Comparative areal distribution of surges at Mt. Pelèe (1902), Lamington (1951), El Chichon (1982) and Bezymianny (1997). The data were extracted from Taylor (1958), Fisher and Heiken (1982), Sigurdsson et al. (1987), and Macias et al. (1997). For El Chichon, only the distribution of the surge S1 is shown. All the surges were generated by collapses of vertical explosive fountains and redirected by the crater topography. The longest axes of all the surge areas are drawn in the same direction (upward). *Closed circle* marks the location of the craters

dispersed radially moving, dense currents which deposited both surge units (S2 and S3) and pyroclastic flows (Macias et al. 1997). However, the earlier S1 surge is interpreted to have occurred from hydromagmatic explosions from the center of the crater, driven by an influx of external water into the magmatic system. We cannot exclude the possibility of infiltration of some meltwater into the magmatic system at Bezymianny. The explosions at El Chichon produced moisture-rich, turbulent pyroclastic surge clouds which were dispersed radially from the volcano with high lateral velocities (Macias et al. 1997). Lamington was interpreted as a similar type of event which originated "directly from crater" (Taylor 1958; Fisher 1979). Useful insights into both of these events, which were not directly observed, and also into the 1997 Bezymianny event may be given by the well-documented episodes of cyclic, Vulcanian explosive activity in 1997 on Montserrat (Druitt et al. 2002). There, transient explosions generated collapse of a semi-circular fountain 300–650 m high which, over a period of ~20 s, generated highly expanded pyroclastic surges which swept down the volcano flanks at frontal velocities of 30–60 m s^{-1}. The surges decelerated 1–2 km from the dome, and then lifted off to form buoyant ash plumes. The limited surge runout on Montserrat was scaled to the relatively small discharge of the explosions which on average involved 3.3×10^5 m^3 DRE of magma – about 30 times less than the 1997 surge at Bezymianny. By contrast, the Lamington surge involved perhaps 5×10^7 m^3 DRE, about five times more than Bezymianny (after data of Taylor 1958, and R.P. Hoblitt, personal communication) and, assuming an explosion of 3–5 min duration, a flux of $2–3\times10^5$ m^3 s^{-1}, roughly three times more than Bezymianny.

Transient numerical modeling of Vulcanian eruptions and column collapse suggests that pyroclastic currents can form within the interior region of an overhanging plume (*overhang* style), or by immediate plume collapse akin to "boiling-over" of gas-charged magma from an open vent (*boil-over* style; Clarke et al. 2002), with the style strongly dependent on the volatile energy available. In the case of Bezymianny, we suggest that the eruption began with the boil-over style of pyroclastic current, forming initially a radial surge, and with the surge reshaped subsequently by the breached crater. Then, after the initial explosive pulse, and with increase in volatiles in the erupting mixture, a transitional behavior developed with simultaneous generation of pyroclastic flows fed by a partly collapsing fountain and a strongly buoyant plume.

An important aspect of the modeling above is its illustration of a near-vent generation of pyroclastic currents for both styles (overhang or boil-over), suggesting that both styles of pyroclastic current would usually be strongly influenced by a breached-crater geometry. The surges of Mt. Pelée, Lamington, El Chichon (S1 surge) and 1997 Bezymianny were all strongly accentuated by the breached-crater topography of their volcanic edifices, a fact which emphasizes the importance of the morphology of the volcanic edifice for volcanic hazard evaluation.

Surge velocity

As discussed above, in many locations a characteristic feature of the deposit surface was the presence of angular, accidental boulder-size clasts which rolled or slid over the deposit surface for considerable distances. Following generally the approach of Clarke and Voight (2000), we develop a simple relation for velocity by equating the force applied to a block by a pyroclastic current to the resisting force mobilized in frictional block sliding.

The relation for minimum cloud speed required to cause sliding (Cs) is

$$Cs = \{2fg/\rho_s C_D\}\left(m/A\right),$$

where g is acceleration of gravity, f is coefficient of sliding friction, ρ_s is density of the current over the height of the moving object, C_D is drag coefficient, m is mass of moving object, and A is frontal area of object. We assume f=0.6 (based on sliding shear tests of crushed andesite tuff on Montserrat; Voight et al. 2002), C_D=1.05 (cube on a flat surface), and ρ_s=0.74 to 4 kg m^{-3} (the former value is for air at 200 °C; the latter values are representative for surges at Unzen and Lamington; Clarke and Voight 2000). For a representative prismatic block of dimensions 23×23×40 cm, m=27.5 kg and A=0.92 cm^2, the velocities required to slide the block are 67 m s^{-1} for an air current, and 29 m s^{-1} for a surge current. The results underscore the significance of entrained particles in raising the cloud density and enabling block sliding to occur at reduced required speeds. Analysis of a limited number of angular blocks suggests minimum required surge cloud speeds of 19–30 m s^{-1}, using the assumptions noted above. By contrast, associated speeds assuming an air current are 44–69 m s^{-1}. We do not insist that the surge densities assumed above are correct, but believe that the analysis yields reasonable order-of-magnitude results. Doubling or halving the assumed densities would change results by root two.

Implications of surge dynamic models

The ash flow model of Bursik and Woods (1996) seems appropriate to describe the sustained current of turbulent particle-laden suspensions, and we examine this model in relation to Bezymianny. The model predicts for a given eruption rate that either a slow and deep subcritical flow or a fast and relatively shallow supercritical flow can develop. The difference between the two states is parameterized by the Richardson number (Ri), which is the ratio between the gravitational force driving the flow and the resulting flow inertia. If Ri>1, the mechanical energy is dominantly potential and the flow regime is subcritical. If Ri<1, energy is dominantly kinetic and flow is supercritical. The initial flow regime depends on the fountain collapse conditions, where Ri decreases with increasing collapse height in response to greater initial speed and mixture dilution.

Subcritical currents propagate with nearly constant volume flux, and their motion and runouts are governed by the air entrained at the source, the sedimentation of particles, and mass eruption rate. After sufficient sedimentation the current becomes buoyant and lifts off to form a co-surge-type of ash cloud, as discussed above for Montserrat. The process of lift-off defines surge runout. By contrast, in energetic supercritical flows, air entrainment decreases mixture density, leading to less extensive flowage deposits and a greater mass of particles in the co-surge ash cloud. The controls on flow regime are complex, as discussed by Freundt and Schmincke (1985), Cole et al. (1993), and Macias et al. (1998), among others.

We consider that the 1997 Bezymianny surge was generated by collapse of a dense jet over a period of 120 s, implying an average mass flux of 8×10^4 m^3 s^{-1}(DRE)$\times$2,600 kg m^{-3}=2×10^8 kg s^{-1}. Given the uncertainties on deposit thickness, co-surge ash volume, and deposits in the crater moat as well as variations in flux, we assume an axysymmetric mass flux for the eruption fountain of 2–4×10^8 kg s^{-1}. The initial mean particle diameter is taken as 400 μm, eruption temperature is taken as 1,000 °K, and fountain radius is 2 km.

For subcritical flow, the Bursik and Woods (1996) model predicts a runout of 8–10 km for a current with 10 wt% volatiles, and log-normal grain-size distributions with variances of 1–4ϕ. In comparison, for supercritical flow runout is 3–4 km for 10 wt% volatiles and, for a similar flow on a 10° slope, runout is 4–5 km. During supercritical flow, air entrainment during the surge causes the current density to decrease more rapidly than by sedimentation alone, and lift-off occurs closer to source.

The 1997 surge went further than predicted simply for supercritical flow, but its runout is superficially compatible with the subcritical flow model. The actual surge current encountered complex topography, such as at the junction of the dome complex and the depositional plain, and quasi-radial channels and ridges, which may have led to a complex mix of flow regimes. A sudden decrease in slope may have promoted development of a hydraulic jump at Bezymianny, which in turn may have caused greater turbulence, air entrainment, and buoyancy. As discussed by Macias et al. (1998), a flow transition would occur from a relatively dense plug or laminar flow to a relatively dilute, turbulent density current, perhaps resulting in an abrupt increase in particle settling speed and rapid deposition of the coarsest pyroclasts. Such a mechanism is consistent with observations of lithic breccias at El Chichon (Macias et al. 1998), but at Bezymianny the valley deposits have been removed by lahars and no direct comparison can be made.

The destruction of the geodetic benchmark frames and movement of large accidental clasts at the base of the surge current indicate current velocities of at least several tens of meters per second, but not necessarily speeds of >100 m s^{-1} suggested by Bursik and Woods (1996) as typical for supercritical flows. However, the estimates are minima, and higher velocities are not precluded. Moderately fast velocities are also suggested by the distribution of debris scattered from destroyed wooden benchmarks, which suggest some influence on the current by local topography. The estimated velocities seem in excess of subcritical flow speeds, generally of the order of 10 m s^{-1}.

A major effect with respect to Bezymianny which is not accounted for in this model is the entrainment of snow into the surge current. Cooling the current by melting of snow and heating and vaporization of water (Sheridan and Wohletz 1983) could suppress buoyancy and enhance supercritical flow runout. Augmented flux by refocused flowage in the 1956 crater could enhance runout. Other factors include the brevity of the explosion, which is near the limit of 100–200 s required to establish steady flow (Bursik and Woods 1996). Also, because sedimentation rate depends on grain size, a smaller mean grain size could produce longer runout. Most of the deposit contains particles in the 0–3ϕ range, with a median diameter around 400 μm, but proximal parts of the deposit are coarser and more poorly sorted (Fig. 11, 12), and the deposit is coarse-tail-graded with distance from source.

Conclusions

The 8–10 May 1997 eruption of the Bezymianny volcano began with slow co-seismic extrusion of a plug at the crest of the lava dome complex. Gravitational failures gradually destroyed the plug and triggered an explosion by decompression of the gas-pressurized conduit. A strong Vulcanian explosion destroyed the top of the dome, with a minimum discharge rate of 8×10^4 m^3 s^{-1} of semi-vesiculated andesitic magma. Immediate gravitational collapse of the fountain (boil-over style of pyroclastic current) generated a powerful pyroclastic surge, which traveled 7 km to the southeast at a speed of (at least) tens of meters per second, and deposited $5–15\times10^6$ m^3 of massive to vaguely laminated, gravelly sand. Its emplacement temperature was <200 °C, possibly reflecting the entrainment of snow and consequential cooling. The asymmetric propagation of the surge was caused by the steep-walled, 1956 collapse crater which focused the flowing pyroclastic mixture towards the southeast. The flow regime was probably supercritical.

The surge was directly followed by the eruption of semi-vesicular, block-and-ash flows generated by fountain collapse, the subangular clasts of which were similar to but slightly less dense than those in the surge. The following fountain-collapse pyroclastic flows became progressively more vesiculated, and the youngest flows of the eruption were characterized by rounded clasts of pumiceous andesite. At this stage the explosive eruption was transitional, involving both a partly collapsing fountain and a buoyant plume. The buoyant plume was of the sub-Plinian type and rose to a height of ~13–14 km. Strong explosive activity lasted about 37 min, and the eruption produced roughly 0.026 km^3 DRE magma (sum of surge, flow and fall) at an average discharge rate of $\sim1.2\times10^4$ m^3 s^{-1}. The evolutionary succession of different eruptive styles of the eruption was caused by changes in the degree of crystallization and vesiculation of magma stored for many months in the conduit of the volcano, and with an "available" volatile content which increased with depth. A fresh batch of volatile-rich magma may have been involved in triggering the new activity. The eruption was consistent with the recent eruptive history at Bezymianny, where since 1956 a distinct periodicity of eruptive activity has been observed (Bogoyavlenskaya and Kirsanov 1981; Alidibirov et al. 1990b). The May 1997 eruption was an exceptional example of the strong eruptions which have occurred every decade or so, when a fresh batch of relatively low-viscosity, siliceous magma of relatively low cristallinity rises to the surface.

Acknowledgements The analyses of pyroclasts and preparation of the manuscript were made during postdoctoral fellowships of A.B. and M.B. at Penn State University. Revisions were made when A.B was supported by an Alexander von Humboldt Fellowship in GEOMAR, Germany. This research was made possible in part by NSF grant 96-14622 and by grant RG1-172 of the U. S. Civilian Research & Development Foundation and Russian Government. Spectrochemical analyses were done by H. Gong at Penn State University. The authors are grateful to the Kamchatka Experimental and Methodical Seismological Department of the Russian Geophysical Survey for providing seismological data. We appreciate the kind assistance of NOAA in Maryland. The paper was improved by the reviews of J.L. Macias, M. Bursik, S. Carey and S. Hughes.

References

Abdurachman EK, Bourdier J-L, Voight B (2000) Nuées ardentes of 22 November 1994 at Merapi volcano, Java, Indonesia. J Volcanol Geotherm Res 100:345–361
Alidibirov M, Dingwell DB (1996) Magma fragmentation by rapid decompression. Nature 380:146–148
Alidibirov M, Dingwell DB (2000) Three fragmentation mechanisms for highly viscous magma under rapid decompression. J Volcanol Geotherm Res 100:413–423
Alidibirov MA, Belousov AB, Kravchenko NM (1990a) The directed blast phase of the eruption of Bezymianny volcano in 1985. Volcanol Seismol 9:798–811
Alidibirov MA, Bogoyavlenskaya GE, Kirsanov IT, Firstov PP, Girina OA, Belousov AB, Zhdanova EYu, Malyshev AI (1990b) The 1985 eruption of Bezymiannyi. Volcanol Seismol 10:839–863
Anilkumar AV, Sparks RSJ, Sturtevant B (1993) Geological implications and applications of high-velocity two-phase flow experiments. J Volcanol Geotherm Res 56:145–160
Belousov AB (1996) Pyroclastic deposits of March 30, 1956 directed blast at Bezymianny volcano. Bull Volcanol 57:649–662
Belousov AB, Belousova MG, Zhdanova EY (1996) Northern group of Kamchatkan volcanoes in 1990–1992. Volcanol Seismol 18:161–170
Belousov AB, Firstov PP, Zhdanova EY (1999) Eruptions of volcano Bezymianny in 1993–1995. Volcanol Seismol 20:321–333
Bogoyavlenskaya GE, Kirsanov IT (1981) Twenty five years of volcanic activity of Bezymianny (in Russian). Volcanol Seismol 2:3–13
Bogoyavlenskaya GE, Braitseva OA, Melekestsev IV, Maximov AP, Ivanov BV (1991) Bezymianny volcano. In: Fedotov SA (ed) Active volcanoes of Kamchatka, vol 1. Nauka, Moscow, pp 166–197
Boudon G, Gourgaud A (eds) (1989) Mount Pelée. J Volcanol Geotherm Res 38:1–200
Braitseva OA, Melekestsev IV, Bogoyavlenskaya GE, Maksimov AP (1991) Bezymiannyi: eruptive history and dynamics. Volcanol Seismol 12:165–195
Bursik MI, Woods AW (1996) The dynamics and thermodynamics of large ash flows. Bull Volcanol 58:175–193
Carey S (1991) Transport and deposition of tephra by pyroclastic flows and surges. In: Sedimentation in volcanic settings. SEPM Spec Publ 45:39–57
Cas RA, Wright JV (1987) Volcanic successions. Modern and ancient. Allen and Unwin, London
Clarke AB, Voight B (2000) Pyroclastic current dynamic pressure from aerodynamics of tree or pole blow-down. J Volcanol Geotherm Res 100:395–412
Clarke AB, Voight B, Neri A, Macedonio G (2002) Transient dynamics of vulcanian explosions and column collapse. Nature 415:897–901
Cole PD, Guest JE, Duncan AM (1993) The emplacement of intermediate volume ignimbrites: A case study from Roccamonfino Volcano, southern Italy. Bull Volcanol 55:467–480
Dingwell DB (1996) Volcanic dilemma: flow or blow? Science 273:1054–1055
Dingwell DB (1998) Recent experimental progress in the physical description of silicic magma relevant to explosive volcanism. In: Gilbert JC, Sparks RSJ (eds) The physics of explosive volcanic eruptions. Geol Soc Lond Spec Publ 145:9–26
Druitt TH (1992) Emplacement of the 18 May 1980 lateral blast deposit ENE of Mount St. Helens, Washington. Bull Volcanol 54:554–572

Druitt T (1998) Pyroclastic density currents. In: Gilbert JC, Sparks RSJ (eds) The physics of explosive volcanic eruptions. Geol Soc Lond Spec Publ 145:145–182

Druitt TH, Young SR, Baptie B, Bonadonna C, Calder ES, Clarke AB, Cole PD, Harford CL, Herd RA, Luckett R, Ryan G, Voight B (2002) Episodes of cyclic vulcanian explosive activity with fountain collapse at Soufriere Hills Volcano, Montserrat. In: Druitt TH, Kokellar BP (eds) The eruption of Soufriere Hills Volcano, Montserrat, from 1995 to 1999. Mem Geol Soc Lond (in press)

Fisher RV (1979) Models for pyroclastic surges and pyroclastic flows. J Volcanol Geotherm Res 6:305–318

Fisher RV, Heiken G (1982) Mount Pelée, Martinique: May 8 and 20, 1902 pyroclastic flows and surges. J Volcanol Geotherm Res 13:339–372

Fisher RV, Schmincke HU (1984) Pyroclastic rocks. Springer, Berlin Heidelberg New York

Fisher RV, Smith AL, Roobol MJ (1980) Destruction of St. Pierre, Martinique, by ash-cloud surges, May 8 and 20, 1902. Geology 8:472–476

Francis P (1993) Volcanoes: a planetary perspective. Clarendon, Oxford

Freundt A, Schmincke H-U (1985) Lithic enriched segregation bodies in pyroclastic flow deposits of Laacher See volcano (E-Eifel, Germany). J Volcanol Geotherm Res 25:193–224

Gardner JE, Thomas RME, Jaupart C (1996) Fragmentation of magma during Plinian volcanic eruptions. Bull Volcanol 58: 144–162

Gardner JE, Hilton M, Carroll MR (1999) Experimental constraints on degassing of magma: isothermal bubble growth during continuous decompression from high pressure. Earth Planet Sci Lett 1668:201–218

Gorshkov GS (1959) Gigantic eruption of the volcano Bezymianny. Bull Volcanol 20:77–109

Hess K-U, Dingwell DB (1996) Viscosities of hydrous leucogranitic melts: A non-Arrhenian model. Am Mineral 81:1297–1300

Hoblitt RP, Harmon RS (1993) Bimodal density distribution of cryptodome dacite from the 1980 Eruption of Mount St. Helens, Washington. Bull Volcanol 55:421–437

Hoblitt RP, Miller CD, Vallance JE (1981) Origin and stratigraphy of the deposits produced by the May 18 directed blast. In: Lipman PW, Mullineaux DR (eds) The 1980 eruptions of Mount St. Helens, Washington. US Geol Surv Prof Pap 1250: 401–419

Hoblitt RP, Wolfe EW, Scott WE, Couchman MR, Pallister JS, Javier D (1996) The preclimactic eruptions of Mount Pinatubo, June 1991. In: Newhall CG, Punongbayan RS (eds) Fire and mud: Eruptions and lahars from Mount Pinatubo, Philippines. Philippine Institute of Volcanology and Seismology, Qezon City, and University of Washington Press, Seattle, pp 457–511

Houghton BF, Wilson CJN (1989) A vesicularity index for pyroclastic deposits. Bull Volcanol 51:451–462

Inman DL (1952) Measures for describing the size distribution of sediments. J Sediment Petrol 22:125–145

Ivanov BV, Kadik AA, Maksimov AP (1978) Physicochemical conditions of crystallization of andesites in the Klyuchevskiy group of volcanoes, Kamchatka. Geokhimiya 8:1139–1155

Kieffer SW (1981) Fluid dynamics of the May 18 blast at Mount St. Helens. In: Lipman PW, Mullineaux DR (eds) The 1980 eruptions of Mount St. Helens, Washington. US Geol Surv Prof Pap 1250:545–570

Lacroix A (1904) La montagne Pelée et ses éruptions. Masson, Paris

Macias JL, Sheridan MF, Espindola JM (1997) Reappraisal of the 1982 eruptions of El Chichon volcano, Chiapas, Mexico: new data from proximal deposits. Bull Volcanol 58:459–471

Macias JL, Espindola JM, Bursik M, Sheridan MF(1998) Development of lithic-breccias in the 1982 pyroclastic flow deposits of El Chichon volcano, Mexico. J Volcanol Geotherm Res 83: 173–196

Moore JL (1967) Base surges in recent volcanic eruptions. Bull Volcanol 30:337–363

Newhall CG, Self S (1982) The Volcanic Explosivity Index (VEI): An estimate of the explosive magnitude for historical volcanism. J Geophys Res 87(C):1231–1238

Ozerov AYu, Demyanchuk YuV, Storcheus AV, Karpov GA (1996) Eruption of Bezymianny volcano, Kamchatka, on October 6–8, 1995. Volcanol Seismol 18:363–367

Seleznev BV, Dvigalo VN, Gusev NA (1984) Evolution of Bezymianny volcano from stereoscopic plotting of aerial photographs of 1950, 1967, 1976–1981. Volcanol Seismol 5:53–66

Sheridan MF, Wohletz KW (1983) Hydrovolcanism. Basic consideration and review. J Volcanol Geotherm Res 17:1–29

Sigurdsson H, Carey SN, Fisher RV (1987) The 1982 eruption of El Chichon volcano, Mexico. 3. Physical properties of pyroclastic surges. Bull Volcanol 49:467–488

Simkin T, Siebert L (1994) Volcanoes of the world. Geoscience Press, Tucson, Arisona

Smith AL, Roobol MJ (1990) Mt Pelee, Martinique. A study of an active island-arc volcano. Geol Soc Am Mem 175

Smithsonian Institution (1996) Global volcanism network. Bulletin 21(8)

Smithsonian Institution (1997) Global volcanism network. Bulletin 22(4)

Sparks RSJ, Walker GPL (1977) The significance of coignimbrite air-fall ashes associated with crystal enriched ignimbrites. J Volcanol Geotherm Res 2:329–341

Sparks RSJ, Bursik MI, Carey SN, Gilbert JS, Glaze LS, Sigurdsson H, Woods AW (1997) Volcanic plumes. Wiley, Chichester

Sparks RSJ, Murphy MD, Lejeune AM, Watts RB, Barclay J, Young SR (2000) Control on the emplacement of the andesite lava dome of the Soufriere Hills Volcano, Montserrat, by degassing-induced crystallization. Terra Nova 12:14–20

Sparks RSJ, Barclay J, Calder ES, Herd RA, Luckett R, Norton GE, Ritchie L, Voight B, Young SR, Woods AW (2002) Generation of a debris avalanche and violent pyroclastic density current on 26 December (Boxing Day) 1997 at Soufriere Hills Volcano, Montserrat. In: Druitt TH, Kokellar BP (eds) The eruption of Soufriere Hills Volcano, Montserrat, from 1995 to 1999. Mem Geol Soc Lond (in press)

Taylor GA (1958) The 1951 eruption of Mount Lamington, Papua. Aust Bur Mineral Resour Geol Geophys Bull 38:1–117

Valentine GA, Fisher RV (2000) Pyroclastic surges and blasts. In: Sigurdsson H (ed) Encyclopedia of volcanoes. Academic, San Diego571–580

Voight B, Sparks RSJ, Miller AD, Stewart RC, Hoblitt RP, Clarke A, Ewart J, Aspinall W, Baptie B, Druitt TH, Herd R, Jackson PP, Lockhart AB, Loughlin SC, Lynch L, Norton GE, Robertson R, Watson IM, Young SR (1999) Magma flow instability and cyclic activity at Soufriere Hills Volcano, Montserrat. Science 283:1138–1142

Voight B, Constantine EK, Siswowidjoyo S, Torley R (2000) Historical eruptions of Merapi Volcano, Central Java, Indonesia, 1768–1998. J Volcanol Geotherm Res 100:69–138

Voight B, Komorowski JC, Norton GE, Belousov AB, Belousova M, Boudon M, Fransis PW, Franz W, Heinrich P, Sparks RSJ, Young SR (2002) The 26 December (Boxing Day) 1997 sector collapse and debris avalanche at Soufriere Hills Volcano, Montserrat. In: Druitt TH, Kokellar BP (eds) The eruption of Soufriere Hills Volcano, Montserrat, from 1995 to 1999. Mem Geol Soc Lond (in press)

Walker GPL (1971) Grain-size characteristics of pyroclastic deposits. J Geol 79:696–714

Walker GPL (1973) Explosive volcanic eruptions – a new classification scheme. Geol Rundsch 62:431–446

Wohletz KH (1998) Pyroclastic surges and compressible two-phase flow. In: Freundt A, Rosi M (eds) From magma to tephra. Elsevier, Amsterdam, pp 247–312

Zharinov NA, Gorel'chik VI, Belousov AB, Belousova MG, Garbuzova VT, Demyanchuk YuV, Zhdanova EY (1991) Volcanic eruptions and seismic activity of Klyuchevskoi, Bezymianny and Shiveluch in 1986–1987. Volcanol Seismol 12(3): 327–345

Zingg T (1935) Beiträge zur Schotteranalyse. Schweiz Mineral Petrol Mitt 15:39–140